

# Label-Free Analysis of DNA Methylation using Optofluidic Ring Resonators

Jonathan D. Suter, *Student Member, IEEE*, Daniel J. Howard, Huidong Shi, Charles W. Caldwell, and Xudong Fan, *Member, IEEE*

**Abstract**— We demonstrate the utility of the opto-fluidic ring resonator (OFRR) sensor for analyzing methylated oligonucleotides. Cytosine methylation, a regular epigenetic function in cellular growth and metabolism, may have ties to abnormal suppression of key genes involved with cellular proliferation. Such behavior is suspected to be strongly related to the occurrence of several types of cancers. The OFRR is demonstrated as a tool both for detecting DNA hybridization and methylated cytosines residues.

## I. INTRODUCTION

DNA methylation is a natural metabolic function that falls under the heading of epigenetic DNA modifications. Broadly speaking, these are modifications which cause changes in gene function that cannot be explained by changes in DNA sequence [1].

Over the past several years, numerous studies have unearthed evidence for the connection between abnormal genomic methylation and certain types of cancers [2-4]. Located mostly in CpG islands, methylated nucleotides help cells regulate protein transcription. When this system behaves abnormally, however, as in hypermethylation, out-of-control gene suppression may lead to dangerous cellular proliferation.

In light of this information, it has become increasingly important for scientists to develop ideal tools for studying and evaluating the degree of methylation in key DNA sequences.

Currently, the workhorse of DNA analysis is the fluorescent microarray, which is capable of single-molecule detection and has well-understood protocols [5, 6]. However, factors such as fluorescence signal bias [7] and analyte labeling procedures make label-free options very attractive for some applications.

We have developed a novel analytical tool for label-free optical biological and chemical detection called the opto-fluidic ring resonator [8]. In the past several years the

performance parameters of this device have been fully explored and applied to many important analytes [8-17]. Very recently, however, the OFRR's ability to detect oligonucleotides has also been intensively investigated [13, 18].

The OFRR, as shown in Fig. 1, is a glass-capillary based cylindrical ring resonator that demonstrates advantages of high sensitivity, low detection limits, small sample volume consumption, and low cost. In optical ring resonators, light circulates repeatedly within a waveguiding closed-loop optical cavity. Photons that match a resonance frequency in the cavity will couple into it. Circular resonances of this kind are described as whispering gallery modes (WGMs). The spectral positions of WGMs are sensitive to the refractive index (RI) of the surrounding media according to the following formula [19],

$$2\pi n_{eff} r = m\lambda, \quad (1)$$

where  $r$  is the ring resonator radius,  $n_{eff}$  is the effective RI experienced by the WGM, and  $m$  is an integer that describes the WGM angular momentum. Using the OFRR as a refractometer, changes in the term  $n_{eff}$  can be caused by two different mechanisms: material immobilization on the interior surface and changes in bulk RI.

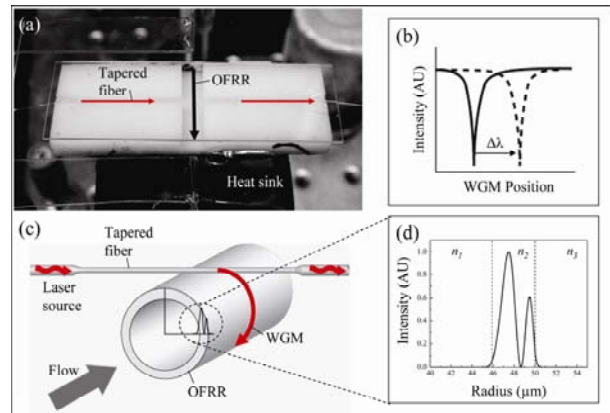


Fig. 1. Photograph of the OFRR platform with capillary and fiber indicated (not otherwise visible) (a), illustration of net WGM shift (b), blown-up schematic of OFRR cross-section (c), and theoretical model of 2<sup>nd</sup> order radial mode intensity across the OFRR wall (boundaries indicated by dotted lines, and  $n_1=1.33$ ,  $n_2=1.45$ ,  $n_3=1.0$ ) (d) (reprinted from [6] with permission from OSA).

Fig. 1(a) shows how the delicate OFRR capillary and fiber elements are aligned on a slotted polymer block. Fig. 1(b) demonstrates how the transmission from the optical

Manuscript submitted April 5, 2009. This work is partially supported by NSF (ECCS-0729903) and the Wallace H. Coulter Foundation Early Career Award. JDS is supported by the NIH Bioterrorism Training Grant.

J. D. Suter, D. J. Howard, and X. Fan are with the Department of Biological Engineering, University of Missouri, Columbia, MO 65211 USA (phone: 573-884-2543; e-mail: fanxud@missouri.edu).

H. Shi is with the Medical College of Georgia Cancer Center, Augusta, GA 30912 USA.

C. W. Caldwell is with the Department of Pathology and Anatomical Sciences, University of Missouri, Columbia, MO 65211 USA.

fiber registers dips corresponding to WGM position, which shift ( $\Delta\lambda$ ) in response to changes in the detected RI. Fig. 1(c) shows a cross-sectional view of the OFRR demonstrating coupling from the optical fiber to the capillary wall. Fig. 1(d) shows an expanded view of 2<sup>nd</sup> order radial modes in the capillary wall. It can be seen how the tail of this distribution extends into the fluid core. This portion of the electric field is referred to as the “evanescent” field. The evanescent field can only be exposed in the core by maintaining very thin walls (<5  $\mu\text{m}$ ).

Using this sensor platform we demonstrate the ability to immobilize ssDNA via hybridization and the ability to specifically identify methylated versus non-methylated ssDNA. Methylated ssDNA is immobilized using immunoprecipitation, wherein an antibody specific to methylcytosine nucleotides is first attached to the capillary surface. These results are an important first step in the development of label-free tools for the study of DNA methylation and its role in carcinogenesis.

## II. EXPERIMENTAL METHODS

All oligonucleotides were obtained from either Sigma-Genosys or Integrated DNA Technologies. In these studies, the sequences used are listed in Table 1 below.

TABLE I  
OLIGONUCLEOTIDE SUMMARY

<b>Basic hybridization (25-mer):</b>
Probe strand: 5' – NH <sub>2</sub> -C <sub>6</sub> -CCA ACC AGA GAA CCG CAG TCA CAA T – 3'
Target strand: 5' – ATT GTG ACT GCG GTT CTC TGG TTG G – 3'
Negative control strand: 5' – TAA CAC TGA CGC CAA GAG ACC AAC C – 3'
<b>Methylation (30-mer):</b>
5 methylcytidines per target strand (underlined nucleotides are methylated): 5' – CTG AAC <u>TGT TCC GCC CCA CTG</u> TGA AAG AGC – 3'
Unmethylated negative control strand: 5' – CTG AAC TGT TCC GCC CCA CTG TGA AAG AGC – 3'

Antibody selected was mouse IgG<sub>1</sub> raised against 5-methylcytidine, purchased from AbD Serotec. Dimethyl adipimidate (DMA) crosslinker was obtained from Pierce. Other reagents, including SSC buffer, PBS buffer, ethanol, hydrofluoric acid, 3-aminopropyltrimethoxysilane (3-APS), and protein G were obtained from Sigma-Aldrich. OFRR capillary performs were purchased from Sutter Instruments. Water, used as a diluent or in buffers, was purified to 18 M $\Omega$  using a Barnstead Easypure-UV system.

The OFRR is fabricated from a quartz glass capillary with an initial outer diameter of 1.2 mm and wall thickness of 150  $\mu\text{m}$ . Focused CO<sub>2</sub> lasers soften the capillary preform, and it is then pulled until the outer diameter is approximately 100  $\mu\text{m}$  and the wall thickness is approximately 5  $\mu\text{m}$ . Once connected to polymer tubing, hydrofluoric acid (HF) is passed through the capillary,

etching the wall down even further. The wall thickness is estimated using a theoretical model described previously [8, 16] and is monitored until the bulk refractive index sensitivity (BRIS) reaches an appropriate benchmark, which in these experiments was either 6.8 nm/RIU or 51.9 nm/RIU. Fig. 2 shows how these BRIS values were measured, using serial dilutions of ethanol in water.

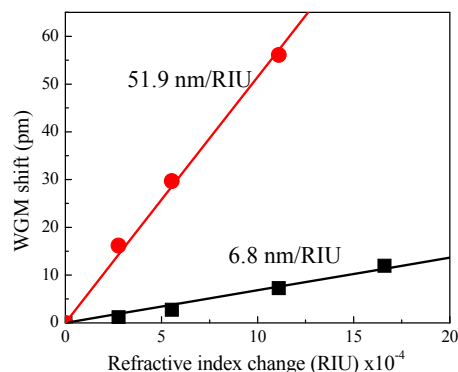


Fig. 2. Bulk refractive index sensitivity (BRIS) measurement using ethanol dilutions in water for two different OFRR capillaries.

For stability, the capillary and tapered optical fiber were fixed into grooves on a PVC or polyethylene rectangle and connected to external fluidic and optical components (photographed in Fig. 1(a)). These grooves were covered with a glass slide to insulate the components from ambient air currents. The whole module was then placed on top of a thermal electric cooling (TEC) unit from Marlow Industries which was connected to a high precision temperature controller (ILX Lightwave). This ensured long term temperature stability down to  $\pm 0.01^\circ\text{C}$ . All experiments were performed close to room temperature. A digital syringe pump kept fluid circulating through the OFRR at a constant rate of 10  $\mu\text{L}/\text{min}$ .

The optical input is generated by a continuous wave tunable laser operating at around 1550 nm. It is tuned through a spectral range of approximately 100 pm at a rate of 2 Hz. The fiber taper described above guides this light to the OFRR capillary with which it evanescently interacts. The end of the tapered fiber leads to an infrared photodetector. A custom Labview program monitors the WGM spectrum in real time, acquiring spectra at a rate of 2 Hz.

## III. RESULTS

As a preliminary effort, the OFRR's response to basic hybridization was characterized. Fig. 3(a) shows the net shifts over time for immobilization of 25-mer probe ssDNA (step “B”). This involves covalently binding the aminated probe ssDNA to the silanized glass surface using DMA, followed by complementary target ssDNA (step “C”). Prior to step “A,” the OFRR had already been treated with 3-APS to provide surface amine groups, the procedures for which are described previously [13]. The concentration of the probe and target oligonucleotides was 10  $\mu\text{M}$ . The

triangular data points indicate a negative control where the completely non-complementary target strand was used. The shift for the negative control was approximately 2 pm. Note that the BRIS for this experiment was measured at 6.8 nm/RIU, which is much lower than in the immunoprecipitation experiment. This curve shows that a large signal shift from hybridization can be obtained, even using an OFRR with relatively low sensitivity. Also, the hybridization efficiency for this run appears to be around 30%, consistent with previous studies. In previous OFRR DNA studies, efficiencies closer to 50% have been observed [13].

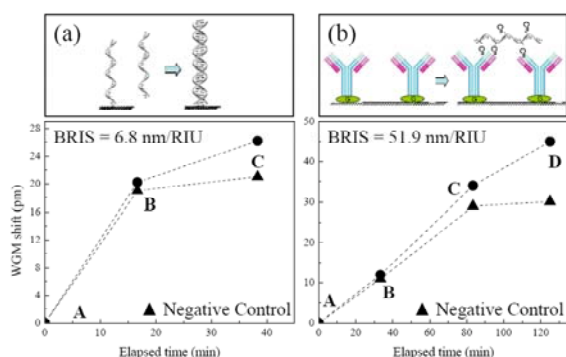


Fig. 3. Net WGM shift for hybridization of 25-mer complementary target (A: initial baseline, B: 10  $\mu$ M probe immobilization, C: 10  $\mu$ M target hybridization) (a). Net WGM shift for immobilization of 30-mer target oligonucleotide with 5 methylated cytosines to antibody (A: initial baseline, B: protein G deposition, C: antibody immobilization, D: 10  $\mu$ M target immobilization) (b).

Fig. 3(b) shows the net WGM shift for the immobilization of methylated ssDNA with 5 methylated cytosines per strand. The concentration of this target ssDNA was also 10  $\mu$ M. In this phase of the study, higher BRIS was sought out in order to study the relatively poorly understood interaction between methylcytosines and the 5-methylcytosine antibody. Before step "A" in Fig. 3(b), the OFRR had already been treated with 3-APS. Step "B" represents covalent immobilization of protein G using DMA as a crosslinker, which attracts antibodies in step "C." Step "D" represents the final net shift for captured ssDNA molecules. Again, the triangular data points represent a negative control. The negative control strand, in this case, was an ssDNA strand without any methyl groups, which generated a WGM shift of approximately 1.1 pm. Fig. 3(b) shows the validity of this test for capturing methylated ssDNA with high specificity.

#### IV. CONCLUSION

The analysis of abnormal epigenetic patterns in key gene sequences is an important frontier in modern cancer research. The OFRR, capable of sensitivities of over 51.9 nm/RIU, has been demonstrated as a label-free methylation-specific sensor. Its capabilities for immobilizing DNA via both hybridization and immunoprecipitation have been

established. Future efforts will focus on developing arrays for methylation analysis built into a lab-on-a-chip platform offering greater integration of optical and fluidic components. Also, the affinity chemistries will be further researched to find solutions for sequence-specific analysis in mixed solutions.

#### REFERENCES

- [1] V. E. A. Russo, R. A. Martienssen, and A. D. Riggs, *Epigenetic mechanisms of gene regulation*. Cold Spring Harbor, NY: Cold Spring Harbor Laboratory Press, 1996.
- [2] P. A. Jones and S. B. Baylin, "The fundamental role of epigenetic events in cancer," *Nat. Rev. Genet.*, vol. 3, pp. 415-428, 2002.
- [3] G. Egger, G. Liang, A. Aparicio, and P. A. Jones, "Epigenetics in human disease and prospects for epigenetic therapy," *Nature*, vol. 429, pp. 457-463, 2004.
- [4] J. G. Herman, A. Umar, K. Polyak, J. R. Graff, N. Ahuja, J.-P. J. Issa, S. Markowitz, J. K. V. Willson, S. R. Hamilton, K. W. Kinzler, M. F. Kane, R. Kolodner, B. Vogelstein, T. A. Kunkel, and S. B. Baylin, "Incidence and Functional Consequences of hMLH1 Promoter Hypermethylation in Colorectal Carcinoma," *P. Natl. Acad. Sci. USA*, vol. 95, pp. 6870-6875, 1998.
- [5] R. S. Gitan, H. Shi, C.-M. Chen, P. S. Yan, and T. H.-M. Huang, "Methylation-Specific Oligonucleotide Microarray: A New Potential for High-Throughput Methylation Analysis," *Genome Res.*, vol. 12, pp. 158-164, 2002.
- [6] F. V. Jacinto, E. Ballestar, and M. Esteller, "Methyl-DNA immunoprecipitation (MeDIP): Hunting down the DNA methylome," *Biotechniques*, vol. 44, pp. 35-43, 2008.
- [7] W. G. Cox and V. L. Singer, "Fluorescent DNA hybridization probe preparation using amine modification and reactive dye coupling," *Biotechniques*, vol. 36, pp. 114-122, 2004.
- [8] I. M. White, H. Oveys, and X. Fan, "Liquid-core optical ring-resonator sensors," *Opt. Lett.*, vol. 31, pp. 1319-1321, 2006.
- [9] I. M. White, J. Gohring, and X. Fan, "SERS-based detection in an optofluidic ring resonator platform," *Opt. Express*, vol. 15, pp. 17433-17442, 2007.
- [10] G. Yang, I. M. White, and X. Fan, "An opto-fluidic ring resonator biosensor for the detection of organophosphorus pesticides," *Sensor Actuat. B-Chem.*, vol. 133, pp. 105-112, 2008.
- [11] H. Zhu, I. M. White, J. D. Suter, and X. Fan, "Phage-based label-free biomolecule detection in an opto-fluidic ring resonator," *Biosens. Bioelectron.*, vol. 24, pp. 461-466, 2008.
- [12] J. D. Suter, I. M. White, H. Zhu, and X. Fan, "Thermal characterization of liquid core optical ring resonator sensors," *Appl. Opt.*, vol. 46, pp. 389-396, 2007.
- [13] J. D. Suter, I. M. White, H. Zhu, H. Shi, C. W. Caldwell, and X. Fan, "Label-free quantitative DNA detection using the liquid core optical ring resonator," *Biosens. Bioelectron.*, vol. 23, pp. 1003-1009, 2008.
- [14] I. M. White, H. Zhu, J. D. Suter, N. M. Hanumegowda, H. Oveys, M. Zourob, and X. Fan, "Refractometric Sensors for Lab-on-a-Chip Based on Optical Ring Resonators," *IEEE Sens. J.*, vol. 7, pp. 28-35, 2007.
- [15] H. Zhu, I. M. White, J. D. Suter, P. S. Dale, and X. Fan, "Analysis of biomolecule detection with optofluidic ring resonator sensors," *Optics Express*, vol. 15, pp. 9139-9146, 2007.
- [16] H. Zhu, I. M. White, J. D. Suter, M. Zourob, and X. Fan, "Integrated Refractive Index Optical Ring Resonator Detector for Capillary Electrophoresis," *Anal. Chem.*, vol. 79, pp. 930-937, 2007.
- [17] H. Zhu, I. M. White, J. D. Suter, M. Zourob, and X. Fan, "Opto-fluidic micro-ring resonator for sensitive label-free viral detection," *Analyst*, vol. 133, pp. 356-30, 2008.
- [18] J. D. Suter, D. J. Howard, H. Shi, C. W. Caldwell, and X. Fan, "Label-free methylation analysis using DNA immunoprecipitation within an opto-fluidic ring resonator," *The Analyst*, vol. In press, 2009.
- [19] M. L. Gorodetsky and V. S. Ilchenko, "Optical microsphere resonators: optimal coupling to high-Q whispering-gallery modes," *J. Opt. Soc. Am. B*, vol. 16, pp. 147-154, 1999.